Fermi National Accelerator Laboratory,
P.O. Box 500, Batavia IL, 60510

TD-05-055
12/21/2005

LARP Technology Quadrupole TQC01: 3D Magnetic Design and Analysis

V.V. Kashikhin, A.V. Zlobin

Introduction

LARP Nb_3Sn technology quadrupole models have a goal of demonstrating the field gradient above 200 T/m in a 90 mm aperture and the reproducibility of main magnet parameters. The TQC01 quadrupole design, being developed at Fermilab, is based on 2-layer shell-type coils placed inside the modified mechanical structure of LHC MQXB magnet. TQC01 2D magnetic design and parameters are reported in [1]. This note summarizes the results of the coil end optimization and 3D magnetic analysis.

Magnet cross-section

TQC01 coil cross-section is shown in Figure 1 and the cold-mass cross-section with the flux density distribution in the iron yoke at 13.0 kA is presented in Figure 2.

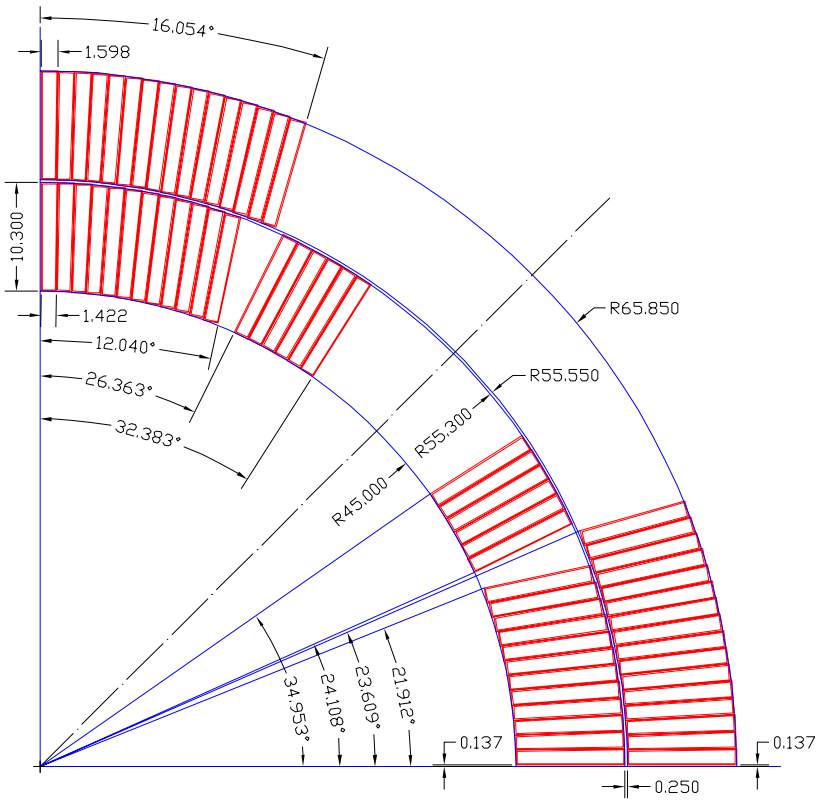

Figure 1. Coil cross-section (dimensions are in [mm]; all dimensions are for the insulated conductors).

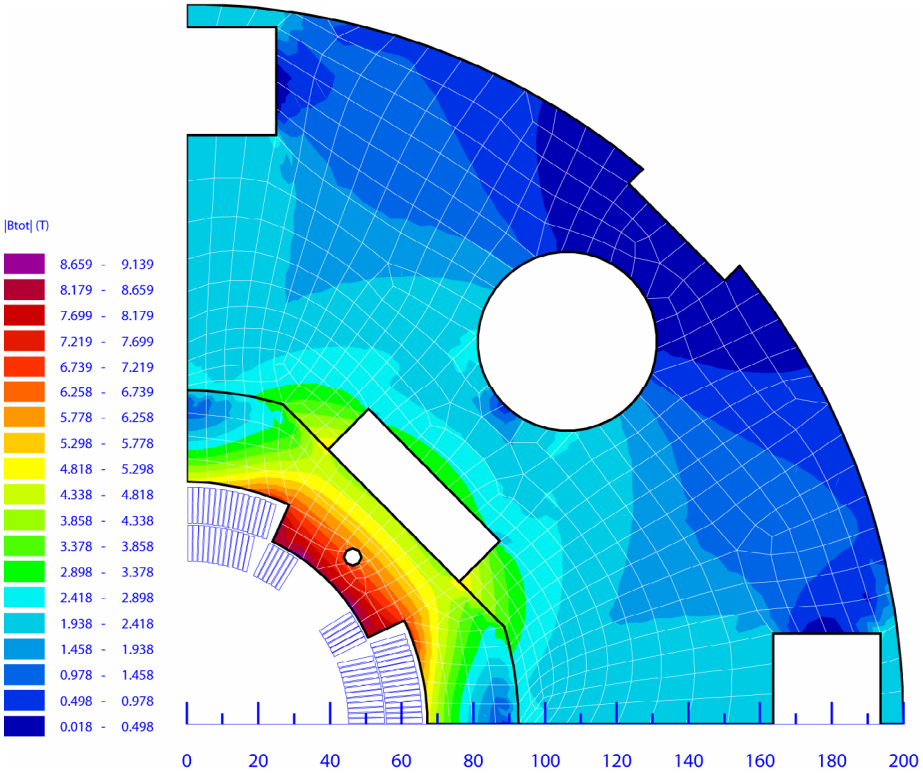

Figure 2. Yoke cross-section with the flux density diagram at 13.0 kA.

TQC01 Rutherford-type cable consists of 27 Nb_3Sn strands, 0.7-mm in diameter. The nominal cable parameters are summarized in Table 1. TQC01 magnet parameters from the 2D magnetic analysis are reported in Table 2 at 4.2 K and 1.9 K.

Table 1. Cable parameters.

Parameter	Unit	Value
№ of strands	-	**27**
Strand diameter	mm	**0.700**
Bare width	mm	**10.050**
Bare inner edge thickness	mm	**1.172**
Bare outer edge thickness	mm	**1.348**
Cabling angle	deg.	**15.5**
Keystoning angle	deg.	**1.000**
Radial insulation thickness	mm	**0.125**
Azimuthal insulation thickness	mm	**0.125**
Copper to non-copper ratio	-	**0.85**

Table 2. Magnet parameters.

Parameter		Unit	Value
N of layers		-	**2**
N of turns		-	**136**
Coil area (Cu + nonCu)		cm^2	**29.33**
Assumed non-Cu J_c at 12 T, 4.2 K		A/mm^2	**2000**
4.2 K temperature			
Quench gradient		T/m	**216.54**
Quench current		kA	**13.027**
Peak field in the coil at quench current		T	**11.233**
Magnet inductance at quench current		mH/m	**4.568**
Stored energy at quench current		kJ/m	**387.60**
Lorentz force per 1st coil octant at quench current	F_x	MN/m	**1.236**
	F_y	MN/m	**-1.828**
1.9 K temperature			
Quench gradient		T/m	**233.14**
Quench current		kA	**14.095**
Peak field in the coil at quench current		T	**12.094**
Magnet inductance at quench current		mH/m	**4.539**
Stored energy at quench current		kJ/m	**450.88**
Lorentz force per 1st coil octant at quench current	F_x	MN/m	**1.388**
	F_y	MN/m	**-2.082**

3D magnetic design

The goal of 3D magnetic design was to define the coil end configurations and the yoke length such that the peak field is reached in the magnet straight section in order to achieve the maximum quench gradient determined in 2D magnetic analysis. At the same time it was required to minimize the length of coil ends to provide the maximum length of the "good" field region for a fixed total magnet length of 40``. Since the block A-lengths and inclination angles in YZ plane play a minor role for the peak field optimization, these parameters were optimized using BEND code for the minimum strain energy during the cable winding [2] and fixed thereafter. The optimum parameters for the three blocks of the coil return end are listed in Table 3 (BL1 – pole block of the inner layer, BL2 – midplane block of the inner layer, BL3 – block of the outer layer).

Table 3. Coil return end geometrical parameters.

Block	A-length, mm	Inclination angle, deg.
BL1	**15**	**8.708**
BL2	**25**	**22**
BL3	**35**	**18**

A 3D magnetic model was built using OPERA 3D code. The block offsets from the coil center were varied together with the iron yoke length for a number of iterations to meet the optimization criteria. Figure 3 shows the initial 3D magnetic model.

The peak field in the coil end B_p^{end} was calculated at 13 kA. The peak field in the magnet straight section at the same current was B_p^{st} = 11.065 T. It is practically independent on the small changes of the coil end design. The B_p^{st} value calculated using the 3D magnetic model is by ~0.15 T smaller than the peak field from 2D magnetic analysis due to the shortness of the magnet.

The peak field increment in the coil ends was defined as $\Delta B_p^{end} = B_p^{end} - B_p^{st}$. Table 4 shows the peak field increments in the coil end with respect to the straight section for eleven end designs with varied iron lengths and block relative positions. The offsets in Table 4 are defined as the distances from the coil center (middle of the 40`` coil) to the ends of the block straight sections or the end of the iron yoke.

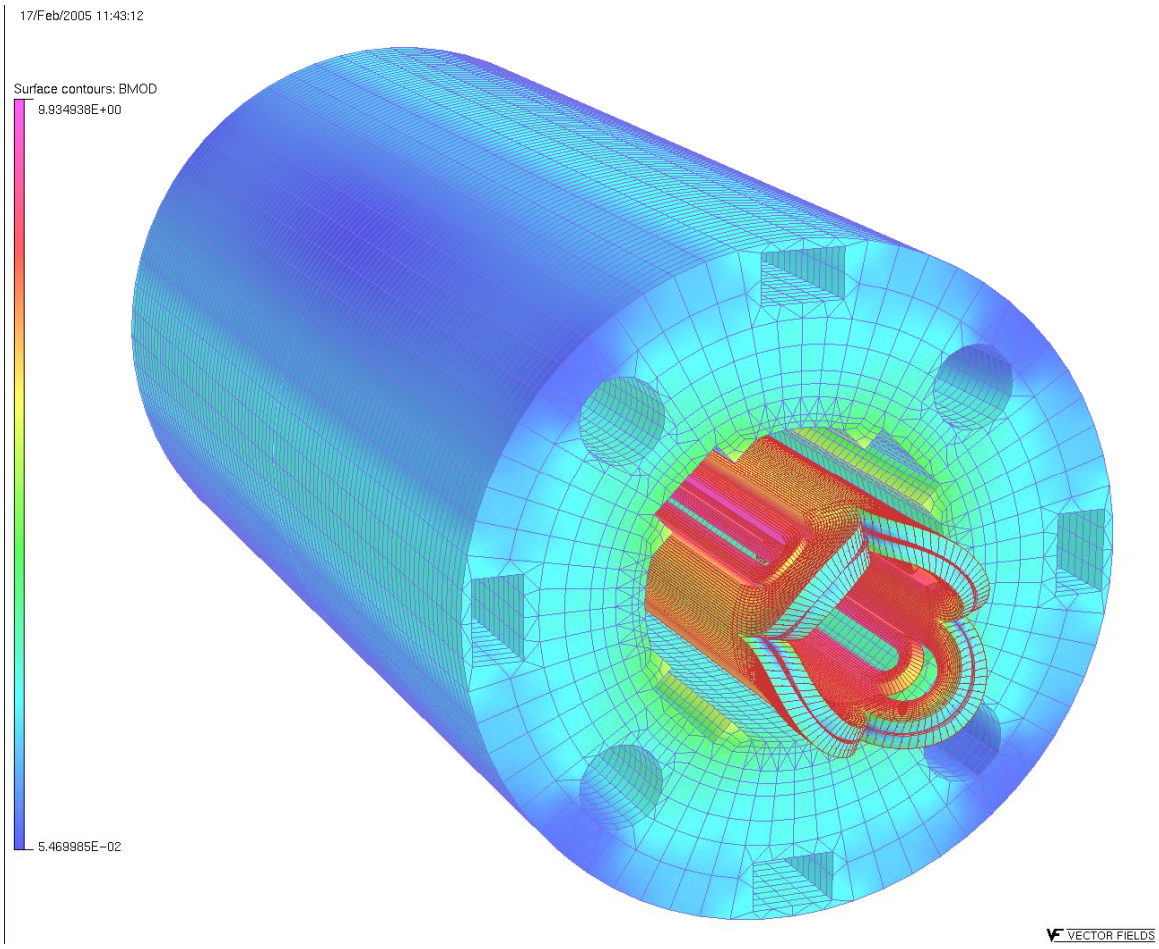

Figure 3. 3D magnetic model.

Table 4. Peak field increment in the coil return end.

Design #	Offsets				ΔB_p^{end}, T		Coil blocks and yoke position
	BL 1	BL 2	BL 3	Yoke	IL	OL	
1	430	440	420	500	**1.60** (14.3%)	-	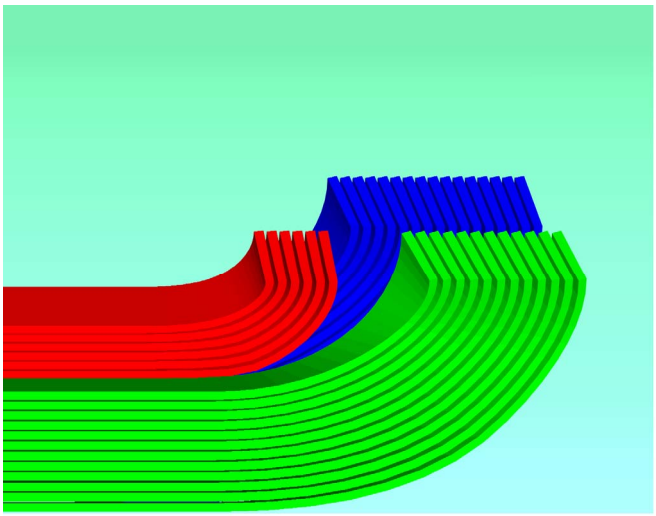
2	420	440	420	500	**1.19** (10.7%)	-	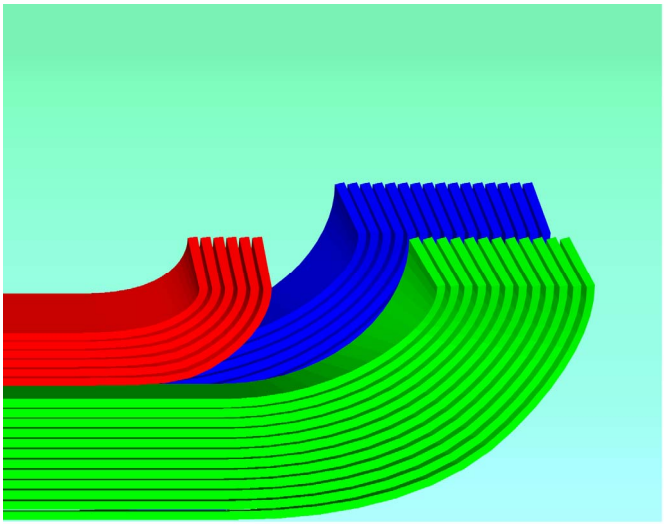

3	410	440	420	500	**0.98** (8.8%)	-	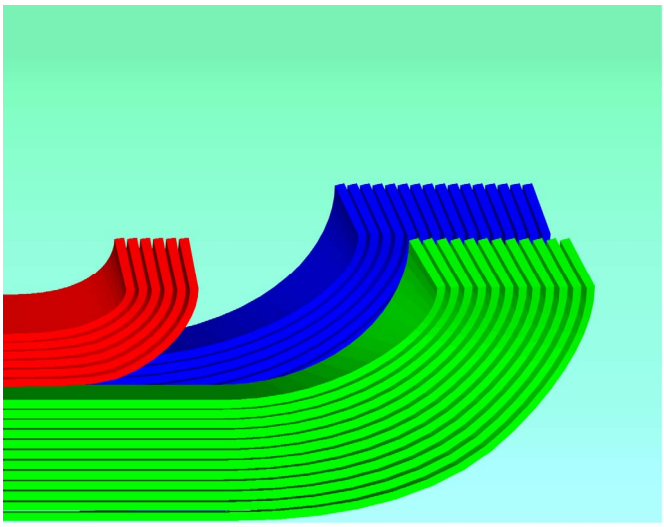
4	400	440	420	500	**0.88** (7.9%)	-	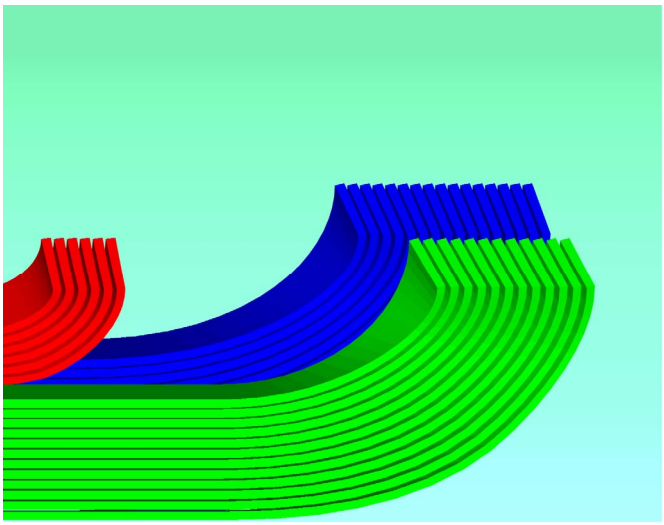
5	430	440	400	500	**0.73** (6.6%)	**0.46** (4.2%)	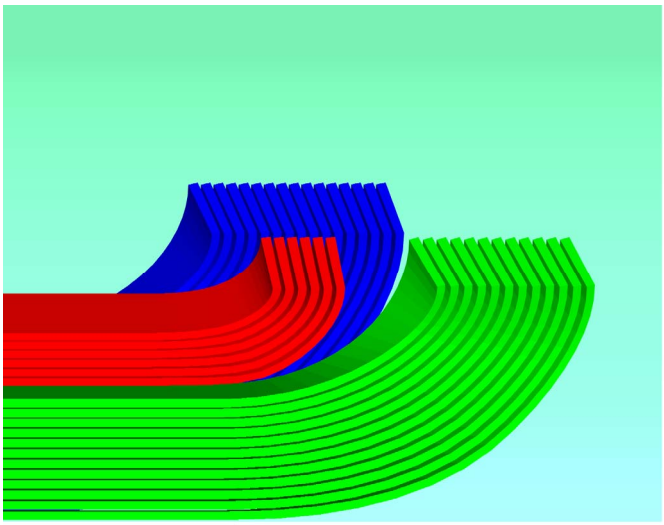

6	430	440	390	500	**-1.49** (-13.5%)	**0.28** (2.5%)	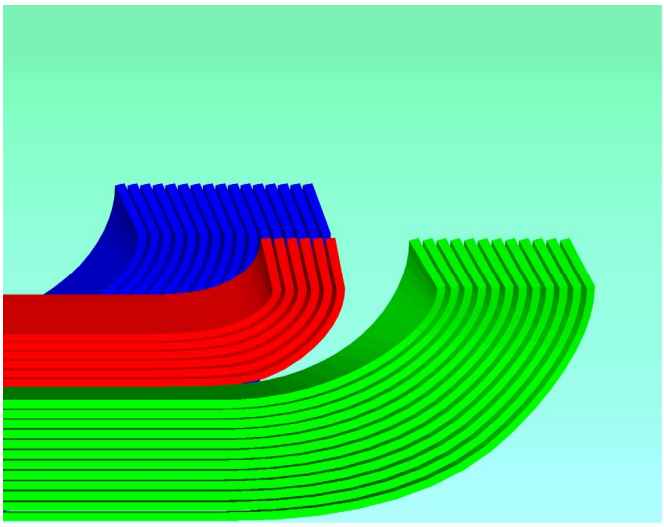
7	430	440	390	380	**-1.89** (-17.1%)	**-0.23** (-2.1%)	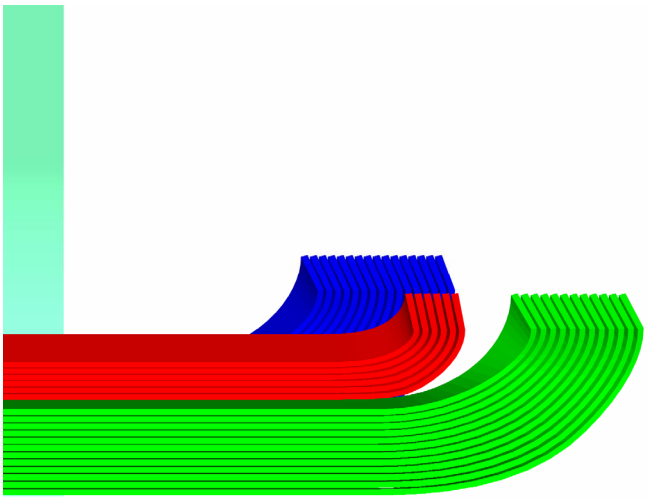
8	410	440	425	365	**-0.05** (-0.46%)	-	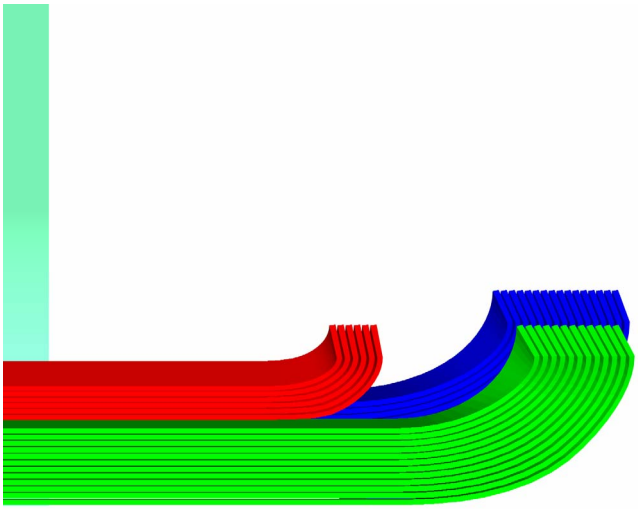

9	400	440	360	350	**-2.15** (-19.4%)	**-0.49** (-4.4%)	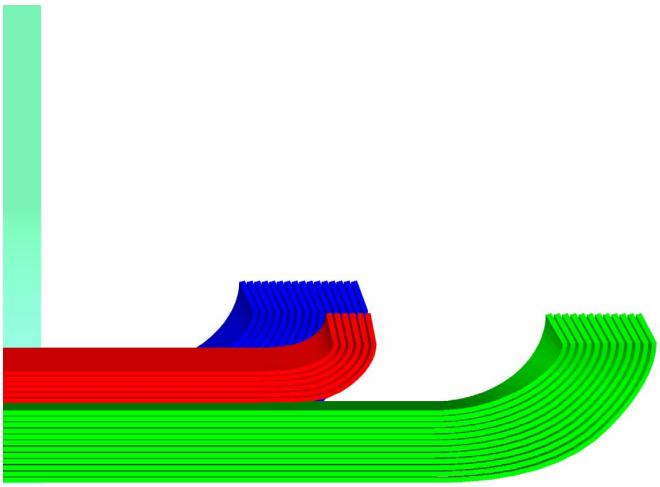
10	400	440	360	360	**-2.11** (-19.1%)	**-0.44** (-4.0%)	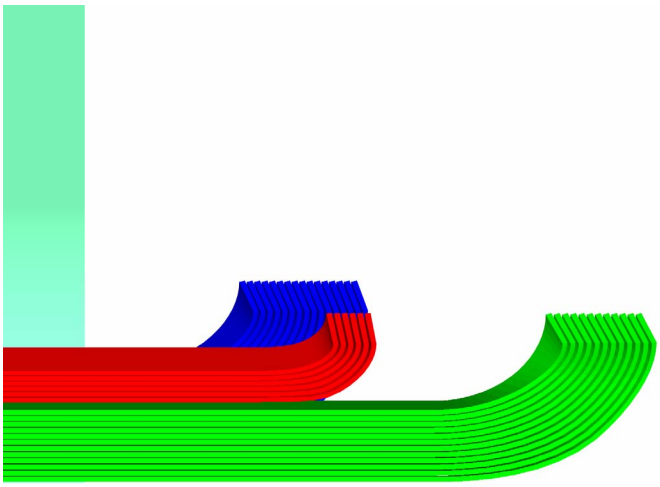
11	400	440	360	370	**-2.07** (-18.7%)	**-0.37** (-3.3%)	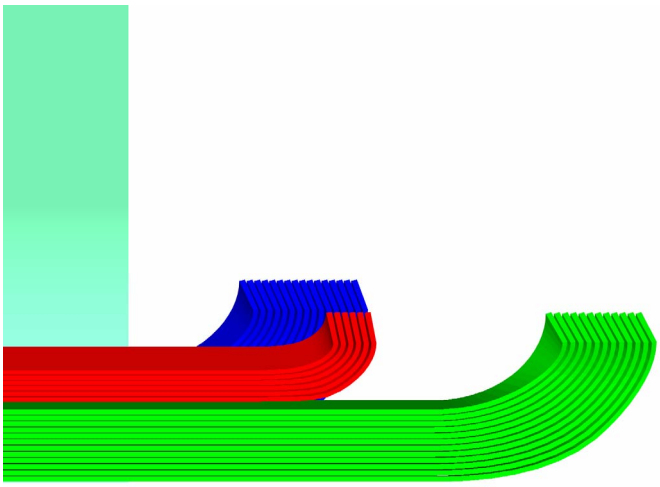

The 3D optimization was started from the most compact end design #1 for the minimum distance between BL1 and BL2 with BL3 extending to the end of the coil that provides the maximum length of the straight section and the iron yoke extending over the coil end. In this case, the peak field in the coil end was 1.6 T (14 %) larger than in the straight section that was clearly unacceptable.

Then in the next three designs #2-#4, the offset of BL1 was gradually reduces, while the positions of the other blocks and iron yoke were not changed. The peak field increment reduced to 0.9 T (7.9 %) for the design #4 and virtually would not change for smaller offsets of BL1. Based on that in the next two design iterations, BL1 was returned to the original position (of design #1) and only the offset of BL3 was gradually reduced.

The peak field became lower in design #5 than in previous cases, although the field started to build up in the outer layer. The peak field increment in design #6 turned negative in the inner layer; however the peak field point moved to the outer layer with the field by 0.3 T (2.5 %) higher than in the straight section. It was close to the ultimate value one could achieve for the iron yoke extending over the coil end since reducing the offset of BL3 even further would not change much the peak field. Thus, the only way to further reduce the peak field in the coil end was to reduce the iron yoke length.

The block positions of design #7 were kept the same as in design #6 and the yoke length was gradually reduced until the peak field increment stopped changing. In this case the coil end was fully extending from the yoke and the peak field in both layers was smaller than in the straight section, although the peak field in the outer layer was by only 0.2 T (2 %) lower than in the straight section.

An attempt to return to the original design concept with BL3 extending to the end of the coil and the maximum distance between BL1 and BL2 (similar to design #4) was made in design #8, however the peak field in the coil end was practically the same as in the straight section. So, given the uncertainty on the cable and block position during the winding it was reasonably safe to proceed with the design #7 for the return end, however a request to equalize lengths of the lead and return ends was made [3] that implied reducing the offset of BL1 (and consequently of BL3) by 30 mm in order to accommodate the transition turn from BL1 to BL2 in the lead end.

At this point the offsets of BL1, BL2 and BL3 were fixed and the next optimization involved only the length of the iron yoke. The distance between the end of the yoke and BL1 (and BL3) in design #9 was set to the same value as in design #7 (that had the minimum yoke length influencing on the peak field). The peak field in the coil end was by 0.5 T (4.4 %) smaller than in the straight section.

In the last two design iterations #10 and #11, the yoke offset was gradually increased with 10 mm steps. There was a small difference in the peak field between designs #9-#11 and any of them can be used for the magnet. Since the yoke length in design #10

happened to be the same as the coil straight section length, it was chosen as the final coil end design. The peak field in the coil lead end will be smaller than in the return end for the same end design due to the interlayer transition turn and was not specifically analyzed. Figures 4-7 show 3D views of the final TQC01 3D magnetic design with the field distributions in the coil and iron yoke.

Note that if necessary for the coil fabrication or other reasons, the offsets listed in Table 4 can be changed. However, it is important that the mutual position of the coil blocks with respect to the yoke end does not change (i.e. the offsets of all the blocks and iron yoke should be changed by the same amount).

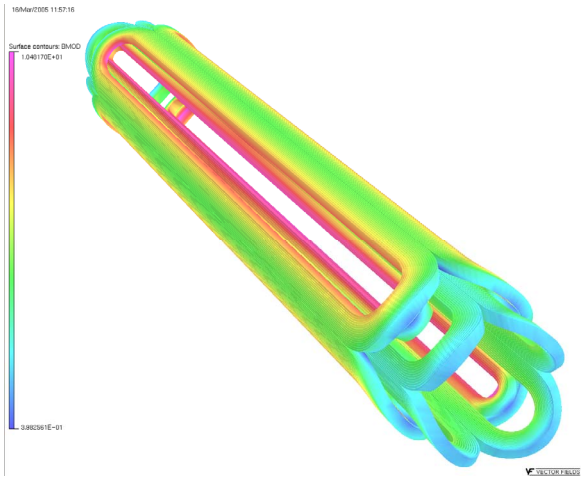

Figure 4. 3D coil view and field distribution.

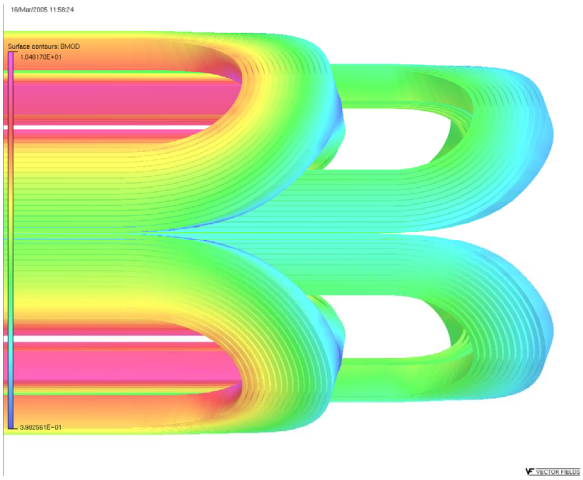

Figure 5. Field distribution in the coil return end.

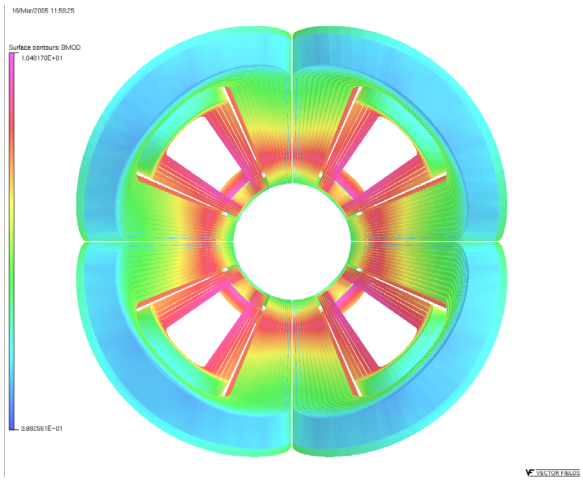

Figure 6. Field distribution on the coil inner surface.

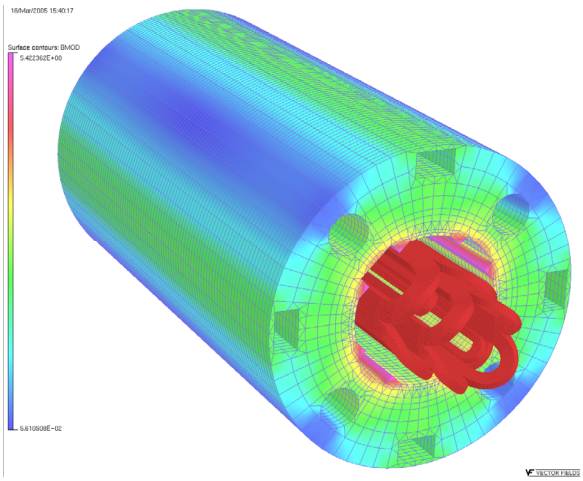

Figure 7. 3D magnet view and field distribution in the iron yoke.

References:

[1] V.V. Kashikhin, A.V. Zlobin, “LARP technology quadrupole TQC01: 2D Magnetic Design and Analysis”, TD-05-052, 12/13/2005.

[2] D. Pasholk, Private communication.

[3] R. Bossert, S. Caspi, P. Ferracin, V.V. Kashikhin, D. Pasholk, FNAL-LBNL teleconference, February 17, 2005.